bio-protocol

Open Access

Published: May 05, 2026

An Advanced Single-Cell RNA Sequencing (scRNA-seq) Protocol Utilizing Custom-Designed Multiplexing

Feng Gao[1], Xujie Liu[1, 2], Fan Sun[2], Yadong Xiao[1, 2], Gutian Xiao[1, 2] and Zhaoxia Qu[1, 2, *]

[1]Department of Immunology and Immune Therapeutics, Hastings Center for Pulmonary Research, Norris Comprehensive Cancer Center, University of Southern California Keck School of Medicine, Los Angeles, CA, USA
[2]Department of Microbiology and Molecular Genetics, UPMC Hillman Cancer Center, University of Pittsburgh School of Medicine, Pittsburgh, PA, USA
*For correspondence: Zhaoxia.Qu@med.usc.edu

Abstract

While cell hashing enhances single-cell RNA sequencing (scRNA-seq) efficiency and minimizes batch effects, commercial mouse hashtags often fail in FVB/N and several other strains due to antibody-epitope incompatibility. We describe a robust alternative utilizing biotinylated antibody cocktails and streptavidin-conjugated oligos to enable reliable sample multiplexing. This approach was validated in FVB/N lung tissues, yielding high-quality single-cell libraries. Our protocol offers a practical solution for researchers requiring strain-specific or custom-designed multiplexing strategies for single-cell transcriptomics.

Key features

- Strain-specific compatibility: Resolves the known H-2^q haplotype mismatch in FVB/N mice that fails standard commercial MHC-I hashtag antibodies in cell hashing.
- Multi-omic 5′ workflow integration: Enables simultaneous sample multiplexing with 10× Genomics 5 chemistry, facilitating joint gene expression and V(D)J repertoire (TCR/BCR) profiling.
- Enhanced non-immune cell labeling: Incorporates anti-CD326 (Ep-CAM) to ensure robust hashing of epithelial and tumor cells that may exhibit MHC-I downregulation or lack CD45.
- Customizable biotin-streptavidin framework: Provides a modular system using biotinylated antibody cocktails and streptavidin-barcodes, adaptable for any mouse strain or tissue-specific cell markers.

Keywords: scRNA-seq, Cell hashing, Sample multiplexing, FVB/N mice, MHC-I haplotype mismatch, 5′ gene expression, Biotin-streptavidin conjugation

This protocol is used in: Frontiers in Immunology (2025), DOI: 10.3389/fimmu.2025.1669117

Graphical overview

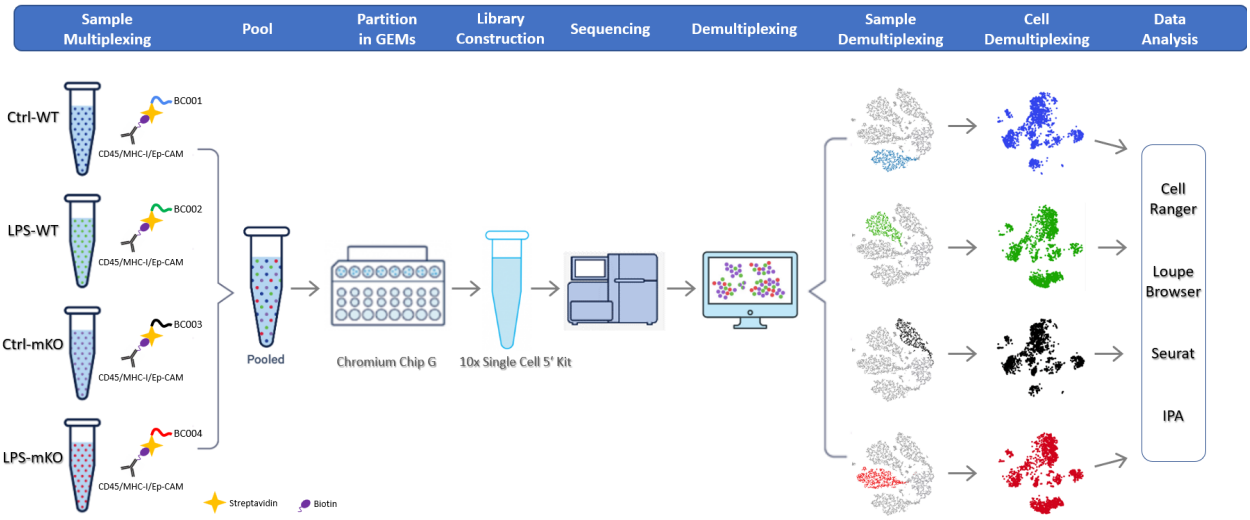

Single-cell RNA sequencing (scRNA-seq) protocol utilizing custom-designed multiplexing

Background

Since its inception in 2009, single-cell RNA sequencing (scRNA-seq) has become an essential technology for profiling the transcriptomic heterogeneity of complex multicellular systems [1]. However, when multiple biological samples are processed in parallel, technical challenges arise, including limited throughput, prohibitive reagent costs, and potential batch effects. Sample multiplexing via cell hashing has emerged as a robust solution to these challenges [2–6]. By labeling individual samples with unique molecular barcodes before pooling and compartmentalization, researchers can integrate multiple samples into a single run, significantly reducing costs while enabling the computational identification and removal of cell doublets or multiplets.

Cell hashing is typically achieved by labeling cell surfaces with oligonucleotide-barcoded reagents, such as oligo-conjugated antibodies targeting ubiquitous surface proteins or lipid/cholesterol-modified oligonucleotides (LMO/CMO) that anchor into the plasma membrane [2–6]. For mouse studies, antibody-based hashing often relies on commercial TotalSeq reagents from BioLegend, which utilize a cocktail of anti-CD45 and anti-MHC Class I (M1/42) antibodies. However, these “universal” reagents are incompatible with the FVB/N and several other mouse strains. Specifically, the M1/42 clone in the commercial mix lacks reactivity with the H-2^{q} haplotype found in FVB/N mice, leading to labeling failure in non-immune (CD45-) populations. Furthermore, while alternative lipid-based multiplexing (e.g., 10× Genomics 3′ CellPlex) approaches are available, they are currently incompatible with single-cell 5′ chemistries, thereby precluding simultaneous profiling of T-cell and B-cell receptor (TCR/BCR) repertoires. The incompatibility of the M1/42 clone is not limited to the FVB/N strain; it also extends to other widely used models carrying the H-2^{q}, H-2^{p}, or H-2^{r} haplotypes, such as the NOD, BUB/BnJ, and RIIIS/J strains. In these genetic backgrounds, standard antibody-based multiplexing often results in the loss of signal in non-immune cell populations, a critical hurdle for lung research where epithelial-immune crosstalk is paramount.

To address these limitations, we developed a versatile cell hashing protocol optimized for the FVB/N strain and compatible with 10× Genomics 5′ workflows [7]. Our method utilizes a customized cocktail of biotin-conjugated antibodies, including anti-CD45 for immune cells, anti-MHC Class I (H-2^{q}) for broad nucleated cell coverage, and anti-CD326 (Ep-CAM) for epithelial and tumor cell enrichment, paired with sample-specific streptavidin-conjugated barcodes. This tripartite antibody approach ensures robust capture of both CD45^{+} immune infiltrates and CD45^{-} parenchymal or malignant cells, the latter of which may exhibit MHC-I downregulation. Here, we provide a detailed, experimentally validated protocol for custom-designed multiplexing and cell hashing to enable high-resolution scRNA-seq on the lung tissues of wild-type (WT) or myeloid *PDLIM2* deletion (mKO) FVB/N mice intratracheally instilled with lipopolysaccharide (LPS) or phosphate-buffered saline (PBS).

The choice of the *PDLIM2*-deficient model for this protocol validation is based on the gene’s critical role in lung homeostasis. *PDLIM2* (PDZ-LIM domain-containing protein 2, also known as SLIM or mystique) is a ubiquitously expressed gene with

the highest level in the lung [8–10]. At the cellular level, *PDLIM2* is expressed abundantly in various epithelial and immune cells, particularly lung epithelial cells and myeloid cells, two functionally critical cell types in the lung [7,10–18]. Not surprisingly, PDLIM2 serves as a vital molecular checkpoint whose repression has been linked to various pathogenic conditions, especially in the lung, such as lung cancer, chronic obstructive pulmonary disease (COPD), interstitial lung disease (ILD)/pulmonary fibrosis (PF), lung infection, and infectious diseases [7,11–16,19–23]. Mechanistically, PDLIM2 acts as a novel ubiquitin ligase enhancer (E5) to stabilize and chaperone the E3 $SCF^{\beta\text{-}TrCP}$ to promote the ubiquitination of nuclear RelA (the prototypical NF-κB member that is also known as p65) and possibly STAT3 and other proteins for proteasomal degradation [24–32]. NF-κB and STAT3 are physiologically vital transcription factors that are tightly regulated, and their persistent activation plays causative roles in various diseases, including lung cancer, COPD, ILD/PF, and infections [33–60]. While it complements existing approaches, the novel scRNA-seq using custom-designed multiplexing is far more advanced in studying NF-κB, STAT3, or any other genes and pathways [61–63].

Materials and reagents

Biological materials

1. Mice: *PDLIM2*$^{flox/flox}$/lysozyme M-Cre$^{+/-}$ mice (mKO) mice were generated as previously described [11,14,16]. Wild-type (WT) control mice were purchased from The Jackson Laboratory (Bar Harbor, ME). All mice were maintained on a pure FVB/N genetic background. For the scRNA-seq experiment, one biological replicate was used per experimental condition (WT-Ctrl, WT-LPS, mKO-Ctrl, and mKO-LPS) and multiplexed into a single library using the described cell hashing protocol.

Reagents

1. Lung Dissociation kit, mouse (Miltenyi Biotec, catalog number: 130-095-927); contains buffer S (20× stock solution), enzyme D (lyophilized powder), and enzyme A (lyophilized powder)
Note: See Recipes for enzyme D and enzyme A preparation before use.
2. Dead Cell Removal kit (Miltenyi Biotec, catalog number: 130-090-101); contains dead cell removal microbeads and 20× binding buffer stock solution
3. Red blood cell lysis solution (10×) (Miltenyi Biotec, catalog number: 130-094-183)
4. Biotin anti-mouse CD45 (BioLegend, catalog number: 103103)
5. Biotin anti-mouse MHC Class I (eBioscience, catalog number: 13-5998-81; clone 34-1-2S), which specifically reacts with the H-2^q haplotype of FVB/N mice, as well as b, s, r, and p haplotypes
6. Biotin anti-mouse Ep-CAM (BioLegend, catalog number: 118203)
7. TotalSeq™-C0951 PE streptavidin (BioLegend, catalog number: 405261)
8. TotalSeq™-C0952 PE streptavidin (BioLegend, catalog number: 405263)
9. TotalSeq™-C0953 PE streptavidin (BioLegend, catalog number: 405265)
10. TotalSeq™-C0954 PE streptavidin (BioLegend, catalog number: 405267)
11. Ethanol (Decon Labs, catalog number: 2701)
12. RPMI-1640 medium (Lonza, catalog number: 12-702F)
13. Sodium chloride (NaCl) (Sigma-Aldrich, catalog number: S9625)
14. Potassium chloride (KCl) (Sigma-Aldrich, catalog number: P9541)
15. Disodium hydrogen phosphate heptahydrate ($Na_2HPO_4 \cdot 7H_2O$) (Fisher Scientific, catalog number: BP331-500)
16. Potassium phosphate monobasic (KH_2PO_4) (Acros Organics, catalog number: 205925000)
17. Bovine serum albumin (BSA) (MP Biomedicals, catalog number: 199898)
18. Dual Index kit TT Set A 96 rxns (10× Genomics, Inc., catalog number: 1000215)
19. Dual Index kit TN Set A 96 rxns (10× Genomics, Inc., catalog number: 1000250)
20. Chromium Next GEM Single Cell 5’ kit v2, 4 rxns (10× Genomics, Inc., catalog number: 1000265)
21. Chromium Next GEM Chip K Single Cell kit, 16 rxns (10× Genomics, Inc., catalog number: 1000287)
22. 5’ Feature Barcode kit, 16 rxns (10× Genomics, Inc., catalog number: 1000256)
23. Trypan Blue (Sigma-Aldrich, catalog number: T8154)
24. Lipopolysaccharide (LPS) (Sigma-Aldrich, catalog number: L2880)

Solutions

1. Phosphate-buffered saline (PBS) (see Recipes)
2. Washing buffer (see Recipes)
3. Labeling buffer (see Recipes)
4. Buffer S (1× solution) (see Recipes)
5. Enzyme D (see Recipes)
6. Enzyme A (see Recipes)
7. Red blood cell lysis solution (1×) (see Recipes)
8. LPS solution (see Recipes)

Recipes

1. PBS

Reagent	Final concentration	Quantity or volume
NaCl	137 mM	8 g
KCl	2.7 mM	0.2 g
$Na_2HPO_4·7H_2O$	10 mM	2.16 g
KH_2PO_4	1.8 mM	0.24 g
H_2O		1,000 mL

To prepare 1 L of 1× PBS, begin by dissolving 8.0 g of NaCl, 0.2 g of KCl, 2.16 g of $Na_2HPO_4·7H_2O$, and 0.24 g of KH_2PO_4 in approximately 800 mL of distilled or Milli-Q water while stirring with a magnetic stir bar. Once the salts are completely dissolved, calibrate a pH meter and adjust the solution to pH 7.4 using a few drops of concentrated HCl (to lower pH) or NaOH (to raise pH), as needed. Finally, transfer the solution to a volumetric flask or graduated cylinder and add distilled water until the total volume reaches exactly 1 L. Then, filter-sterilize (0.22 μm) or autoclave the buffer to prevent microbial growth.

2. Washing buffer

Reagent	Final concentration	Quantity or volume
BSA	0.04%	0.2 g
PBS	1×	500 mL

3. Labeling buffer

Reagent	Final concentration	Quantity or volume
BSA	1%	2 g
PBS	1×	200 mL

4. Buffer S (1×)

Reagent	Final concentration	Quantity or volume
Buffer S (20×)	1×	2 mL
H_2O		38 mL

To prepare 40 mL of 1× buffer S, perform a 1:20 dilution by measuring 2 mL of 20× buffer S and transferring it into a clean container. Add 38 mL of sterile, distilled water to reach the final volume of 40 mL. Mix the solution thoroughly to ensure homogeneity and store the resulting 1× buffer at 2–8 °C until use.

5. Enzyme D

Reagent	Final concentration	Quantity or volume
Enzyme D	1×	1 vial
RPMI-1640		3 mL

Reconstitute the lyophilized enzyme D powder in each vial with 3 mL of RPMI-1640 medium. Close the vial and invert gently for 5 min. Prepare aliquots and store at -20 °C, avoiding freeze/thaw cycles. This solution is stable for 6 months after reconstitution.

6. Enzyme A

Reagent	Final concentration	Quantity or volume
Enzyme A	1×	1 vial
Buffer S (1×)		1 mL

Reconstitute the lyophilized enzyme A powder in the vial with 1 mL of 1× buffer S. Do not vortex. Prepare aliquots and store at -20 °C, avoiding freeze/thaw cycles. This solution is stable for 6 months after reconstitution.

7. Red blood cell lysis solution (1×)

Reagent	Final concentration	Quantity or volume
Red blood cell lysis solution (10×)	1×	5 mL
H_2O		45 mL

Dilute 5 mL of red blood cell lysis solution (10×) with 45 mL of sterile, distilled water.

8. LPS solution

Reagent	Final concentration	Quantity or volume
LPS	5 mg/mL	10 mg
PBS (1×)		2 mL

Stock solutions of LPS at 5 mg/mL are prepared, aliquoted, and frozen at -80 °C to help standardize instillations. Mice are intratracheally instilled with LPS at 4 mg/kg body weight.

Laboratory supplies

1. GentleMACS C tubes (Miltenyi Biotec, catalog number: 130-093-237)
2. Cell strainers, 40 μm (Fisher, catalog number: 22-363-547)
3. Cell strainers, 70 μm (Fisher, catalog number: 22-363-548)
4. Petri dish (Falcon, catalog number: 351029)
5. 35 mm cell culture dish (Greiner Bio-One, catalog number: 627160)
6. MACS MS column (Miltenyi Biotec, catalog number: 130-042-201)
7. 15 mL conical tubes (TH Geyer, catalog number: 7696714)
8. 50 mL conical tubes (Greiner Bio-One, catalog number: 227261)
9. 150 mL vacuum filtration devices, pore 0.22 μm (Jet Biofil, catalog number: FCF010004)
10. 500 mL vacuum filtration devices, pore 0.22 μm (Jet Biofil, catalog number: FPE204500)
11. 2 mL cryovials (Maxxline, catalog number: MLC2B)
12. 5 mL serological pipettes (Greiner Bio-One, catalog number: 606180)
13. 10 mL serological pipettes (Greiner Bio-One, catalog number: 607180)
14. 25 mL serological pipettes (Greiner Bio-One, catalog number: 760160-TRI)
15. Sterile PES syringe filters (Thermo Fisher Scientific, catalog number: 15206869)
16. 50 mL 3-part syringes (Chirana T. Injecta, catalog number: CH03050LL)
17. 10 μL pipette tips (TH Geyer, catalog number: 7695881)
18. 20 μL pipette tips (TH Geyer, catalog number: 7695882)
19. 200 μL pipette tips (TH Geyer, catalog number: 7695884)
20. 1,250 μL pipette tips (TH Geyer, catalog number: 7695887)
21. Countess cell counting chamber slides (Thermo Fisher Scientific, Invitrogen, catalog number: C10283)

Equipment

1. CO_2 chamber
2. Biosafety cabinet
3. Styrofoam board
4. Forceps (Roboz Surgical Instrument, catalog number: RS-5135)
5. Scissors (Roboz Surgical Instrument, catalog number: RS-6802)
6. GentleMACS™ Octo Dissociator with Heaters (Miltenyi Biotec, catalog number: 130-096-427)

Note: Alternatively, a standard GentleMACS™ Dissociator without heating units may be used; in this case, the programmed heating steps must be substituted with manual incubations in a 37 °C water bath for the durations specified in the lung dissociation protocol.
7. Centrifuge (Thermo Fisher Scientific, Thermo Scientific™, model: IEC CL40R, catalog number: 11210927)
8. MACS MultiStand (Miltenyi Biotec, catalog number: 130-042-303)
9. MiniMACS Separator (Miltenyi Biotec, catalog number: 130-042-102) or OctoMACS Separator (Miltenyi Biotec, catalog number: 130-042-109) for use with MACS MS columns
Note: For higher throughput processing, the QuadroMACS™ Separator (supporting up to 4 columns) or the semi-automated MultiMACS™ Cell 24 Separator Plus (supporting up to 24 columns) may be used as alternatives to accommodate larger sample batches.
10. Countess II FL automated cell counter (Invitrogen, catalog number: AMQAF1000)
11. Chromium Controller & Next GEM Accessory kit (10× Genomics, catalog number: 1000202 or 1000204)
12. Thermocycler (Thermo Fisher Scientific, catalog number: 4375786)

Software and datasets

1. Cell Ranger (v7.0): Used for primary data processing, including alignment, filtering, and UMI counting. Available from 10× Genomics (https://support.10xgenomics.com/single-cell-gene-expression/software/pipelines/latest/what-is-cell-ranger)
2. Seurat (v5.0): An R package utilized for secondary analysis, including quality control, normalization, dimensional reduction, and clustering. Available via CRAN or GitHub (https://satijalab.org/seurat/)
3. Ingenuity Pathway Analysis (IPA, QIAGEN): Used for functional enrichment and metabolic pathway analysis of differentially expressed genes. Accessible via QIAGEN Digital Insights (https://digitalinsights.qiagen.com/products-overview/discovery-insights-portfolio/analysis-and-visualization/qiagen-ipa/)
4. Dataset availability: The raw and processed mouse scRNA-seq datasets generated in this study have been deposited in the NCBI Gene Expression Omnibus (GEO) and are publicly available under the accession number GSE249800

Procedure

A. LPS intratracheal instillation in mice

1. Intratracheally instill 6–8-week-old mice with either LPS (4 mg/kg body weight) or an equivalent volume of sterile PBS (control) under light anesthesia. Monitor mice daily for changes in body weight and clinical signs of respiratory distress or systemic inflammation. Typically, symptoms are observed starting on day 2 post-instillation.

B. Preparation of single lung cell suspension

1. Euthanize the mouse by CO_2 inhalation in a CO_2 chamber.
Note: Researchers must strictly adhere to local institutional animal care and use committee (IACUC) guidelines and regional regulations, as CO_2 inhalation protocols may vary or be restricted in certain jurisdictions.

2. Bring the mouse to a biosafety cabinet and dampen it with 70% ethanol.
3. Place the mouse front side up on a dissecting Styrofoam board and fix the arms and legs with needles or tape [64].
4. Use scissors to make an incision in the skin from the abdomen to the neck and tear the skin with forceps to expose the thoracic cage and neck.
5. Carefully cut the ribs to expose the heart and lungs [65].
6. Dissect the lung and remove efferent and afferent blood vessels, trachea, and connective tissue from the lung.
7. Dissect the lung into individual lobes and thoroughly rinse them in a 60 mm × 15 mm Petri dish containing 8 mL of ice-cold PBS. Ensure each lobe is fully submerged during the wash to effectively remove residual blood and surface contaminants.
8. Prepare an enzyme mix by adding 2.4 mL of RPMI-1640 medium, 100 µL of enzyme D, and 15 µL of enzyme A into a 35 mm cell culture dish [66].
9. Transfer the lung lobes to the dish containing the enzyme mix and cut them into 1–2 mm pieces with scissors and forceps.

10. Transfer the tissue pieces and enzyme mix into the gentleMACS C tube (or a sterile 50 mL conical tube if using manual dissociation).
Notes:
1. If a gentleMACS Dissociator is unavailable, manual dissociation can be performed by mincing the tissue into finer pieces using sterile surgical blades, followed by incubation in a 37 °C water bath with constant agitation (e.g., using a magnetic stirrer or orbital shaker) to ensure efficient enzymatic digestion.
2. In case more than one sample from the same treatment group is used, samples from the same treatment group may be pooled before dissociation (see General note 1).

11. Tightly close the C tube and attach it upside down to the sleeve of the gentleMACS Octo Dissociator with Heaters.
Critical: The use of the heater attachment ensures optimal enzymatic activity and consistent tissue digestion; if a heater-equipped dissociator is unavailable, the tube may be incubated in a 37 °C water bath between dissociation programs (see General note 2).

12. Select the gentleMACS Program 37C_m_LDK_1. This automated program consists of a 34-min sequence involving standardized mechanical dissociation steps interspersed with 37 °C incubation periods to optimize enzymatic tissue digestion (see manufacturer's specifications for the Lung Dissociation kit, Mouse).
13. After termination of the program, detach the C tube from the dissociator.
14. Centrifuge the C tube at 300× *g* for 30 s at room temperature and discard the supernatant.
15. Resuspend the sample in 10 mL of RPMI-1640 medium and filter the cell suspension through a 70 μm cell strainer placed over a 50 mL conical tube.
16. Wash the cell strainer with 10 mL of RPMI-1640 medium and combine the wash with the cell suspension from step B15.
17. Centrifuge the cell suspension at 300× *g* for 10 min at room temperature. Aspirate the supernatant completely.
18. Resuspend the cell pellet in 1 mL of 1× red blood cell lysis solution and incubate on ice for 10 min.
19. Add 10 mL of washing buffer to terminate lysis and centrifuge at 300× *g* for 10 min at 4 °C.
20. Resuspend the cell pellet in 10 mL of washing buffer and count cells using a Countess™ II Cell Counter.

C. Cell hashing

1. Transfer the cell suspension containing 1×10^7 cells to a 50 mL conical tube and centrifuge at 300× *g* for 10 min at 4 °C.
2. Prepare the antibody cocktail by adding 1 mL of labeling buffer and 2.5 μg of each biotinylated antibody per sample (anti-CD45, anti-EpCAM, and anti-MHC class I).
Critical: Ensure the anti-MHC class I antibody used (e.g., clone 34–1-2S) is specifically reactive with the H-2^q haplotype of the FVB/N mouse; standard commercial MHC-I clones (such as M1/42) lack this reactivity and will result in labeling failure of non-immune cells.

3. Resuspend the cell pellet in 1 mL of the antibody pool by gently pipetting up and down at least five times using a P1000 tip to ensure a homogeneous suspension. Incubate the mixture for 30 min at 4 °C with continuous gentle rotation (e.g., using a tube rotator at 10–20 rpm) to prevent cell settling and ensure uniform antibody binding.
4. Centrifuge samples at 400× *g* for 5 min at 4 °C. Carefully aspirate the supernatant using a P1000 pipette tip, holding the tube at an oblique angle to avoid disturbing the cell pellet. Resuspend the pellet in 1 mL of cold labeling buffer by gentle pipetting or flicking the tube. Repeat this wash process two additional times for a total of three washes.
5. Resuspend each cell pellet in 1 mL of labeling buffer containing 1.2 μg of the unique TotalSeq™-C oligo-barcoded streptavidin. Ensure a homogeneous suspension by gently pipetting with a P1000 tip at least five times. Incubate the suspension for 20 min at 4 °C with continuous gentle rotation to prevent cell settling and ensure uniform antibody binding.
Critical: Ensure each biological sample is labeled with a unique streptavidin-conjugated oligo barcode (see General note 3).

6. Centrifuge samples at 400× *g* for 5 min at 4 °C. Then, wash three times with 1 mL of labeling buffer as in step C4.

D. Dead cell removal

1. Prepare 1× binding buffer by diluting the 20× binding buffer stock solution (supplied with the Dead Cell Removal kit) with sterile, double-distilled water (ddH2O) at a 1:20 ratio.
2. Resuspend the cell pellet from step C6 in 100 μL of dead cell removal microbeads.

Critical: The volume of dead cell removal microbeads should be maintained as specified for any cell load up to 10^7 cells (see General note 4).

3. Mix well by gentle pipetting and incubate for 15 min at room temperature (20–25 °C) under static conditions.
Critical: Do not use a rotator or vortex during this incubation. The microbeads are in a colloidal suspension and do not settle; therefore, active agitation is neither required nor recommended. Such agitation may negatively impact cell recovery, whereas static incubation ensures consistent labeling (per manufacturer's technical specifications for kit 130-090-101).

4. Add 1× binding buffer to the cell suspension to reach a minimum volume of 500 µL for MACS MS column separation.
5. Filter the cell suspension through a 40 µm cell strainer.
6. Place an MS column in the magnetic field of a suitable MACS Separator.
7. Prepare the column by rinsing with 0.5 mL of 1× binding buffer.
8. Apply the cell suspension onto the column reservoir and collect the flowthrough, which contains the unlabeled (live) cells, while the magnetically labeled dead cells are retained within the column.
9. Wash the column three times with 0.5 mL of 1× binding buffer each. Collect the unlabeled cells that pass through and combine with the flowthrough from step D8.
10. Centrifuge the combined effluents at 300× *g* for 10 min at 4 °C.
11. Wash the cells three times with 1 mL of washing buffer each.
12. Resuspend the cell pellet in 200 µL of washing buffer and count the cells using Trypan Blue by Countess® II Cell Counter.
13. (Optional) If the live cell fraction is less than 90%, repeat the dead cell removal procedure as described in steps D2–11 with a new column.
Pause point: The experimental phase concludes here. All subsequent steps involve computational analysis of the acquired data.
Note: See General note 5 for the integration of biological replicates.

E. GEM generation and library construction

1. Dilute each sample from step C12 in washing buffer to a final concentration of 1×10^6 cells/mL (1,000 cells/µL).
2. Combine 200 µL of labeled cells from each sample in a tube and mix well for gel beads-in-emulsion (GEMs) generation.
3. Perform GEM generation and construction of the 5′ gene expression and cell hashing libraries according to the Chromium Next GEM Single Cell 5’ Reagent kits v2 (Dual Index) User Guide with Feature Barcode technology for Cell Surface Protein & Immune Receptor Mapping (10× Genomics, CG000330 Rev A).
4. Perform sequencing of the libraries according to the guidelines in the user guide.

Data analysis

Following library preparation, the gene expression and cell hashing libraries were sequenced on an Illumina NovaSeq S4 platform using paired-end reads, aiming for a depth of 250 million and 50 million reads, respectively. Raw sequencing data were processed using the 10× Genomics Cell Ranger pipeline (v7.0) to perform demultiplexing, read alignment, and cellular barcode/UMI quantification. The resulting feature-barcode matrices were then imported into the Seurat R package (v5.0) for downstream analysis.
Initial quality control was performed to exclude low-quality cells based on a minimum threshold of 500 UMIs and 200 detected features (genes) per cell. Cells with a mitochondrial gene content exceeding 12% were filtered out to remove apoptotic or damaged cells. After batch effect correction, the data underwent dimensionality reduction and unsupervised clustering. Samples were demultiplexed on biotin-streptavidin hashtag barcodes (Figure 1). Cell types were annotated based on the expression of canonical markers (Figure 2). Differential gene expression was assessed to identify differentially expressed genes (DEGs) at both the cluster and sample levels. Finally, these DEGs were analyzed using Ingenuity Pathway Analysis (IPA, QIAGEN) to identify significantly enriched biological pathways and functional networks (Figure 3).

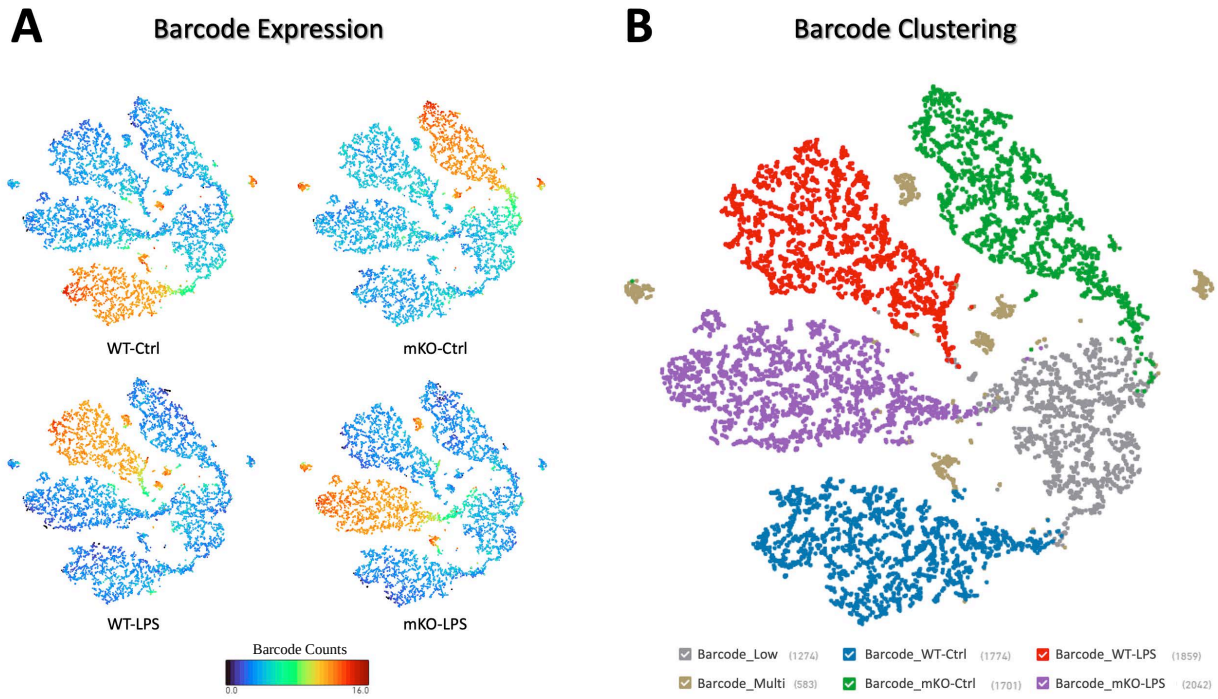

Figure 1. Validation of custom cell hashing and sample demultiplexing in FVB/N mice. (A) UMAP illustrating the specific signal intensity of each biotin-streptavidin hashtag barcode across the four experimental groups: WT-Ctrl, WT-LPS, mKO-Ctrl, and mKO-LPS. (B) UMAP visualization of the barcode clusters, demonstrating distinct separation of the four pooled samples and minimal cross-sample contamination, confirming high demultiplexing accuracy.

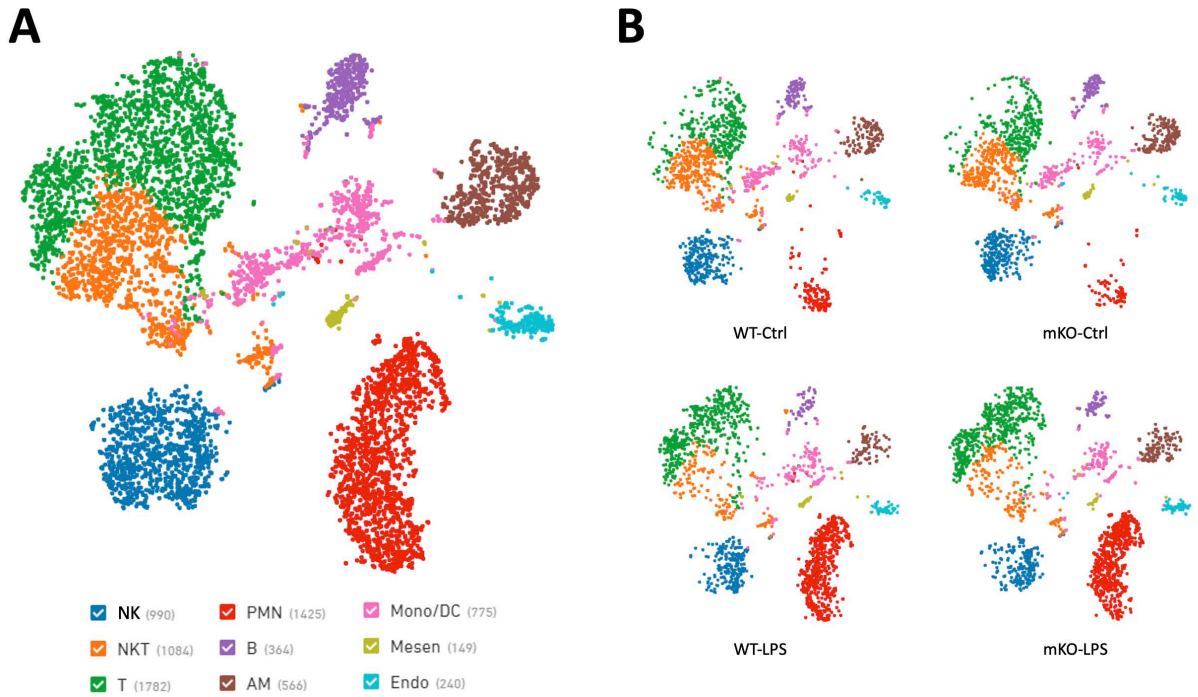

Figure 2. Cellular landscape and clustering of the FVB/N lung with and without lipopolysaccharide (LPS) exposure. (A) Integrated UMAP embedding of all barcode-certified cells from all four experimental groups (WT-Ctrl, WT-LPS, mKO-Ctrl, and mKO-LPS), colored by identified cell types. (B) Split-UMAP projections of the four experimental groups demonstrating consistent cell-type representation and shifts in cell population density (e.g., neutrophil recruitment) following LPS instillation in both WT and mKO strains.

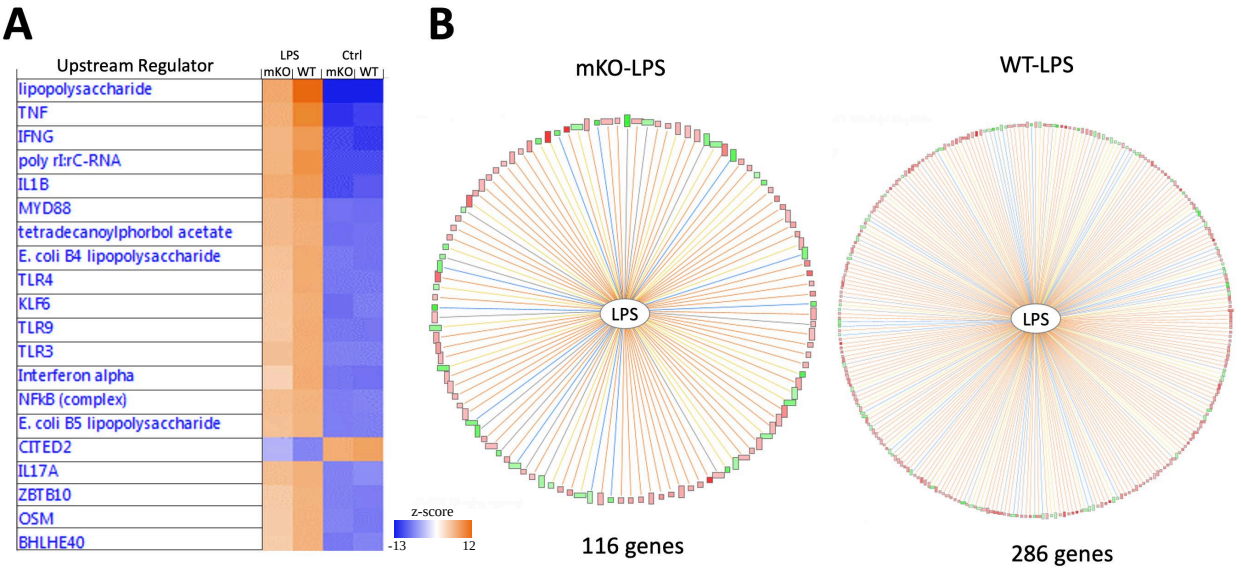

Figure 3. Upstream regulator analysis validating the biological response to lipopolysaccharide (LPS) administration. (A) Ingenuity pathway analysis (IPA), identifying LPS and its downstream signaling hubs (e.g., *TNF*, *IL1B*) as the top-ranked upstream regulators based on the differential gene expression. (B) Radial regulation diagram, showing the predicted activation states and directional relationships between LPS and target molecules. Red/green nodes indicate observed up/down-regulation, while orange/blue lines represent predicted activation/inhibition connections. The attenuated gene activation in mKO mice reveals an impaired immune response following *Pdlim2* deletion, demonstrating the protocol's sensitivity in deconvoluting strain-specific mechanisms of action from a single multiplexed run.

Validation of protocol

This protocol has been used and validated in the following research article:

- Gao et al. [7]. Myeloid *PDLIM2* repression as a common mechanism of infection susceptibility in lung diseases. *Front. Immunol*. 2025;16:1669117 (Figures 3–5, Supplemental figures 1–2).

In summary, this protocol was functionally validated by resolving the lung microenvironments of FVB/N mice across four distinct experimental conditions. By utilizing a custom biotinylated antibody cocktail combined with streptavidin-conjugated oligos, we successfully demultiplexed over 7,000 cells with high signal-to-noise ratios and minimal doublet interference. The biological accuracy of the method was confirmed by three key metrics: (1) the identification of all major lung cell populations; (2) the robust detection of canonical LPS-responsive upstream regulators; and (3) the successful characterization of the compromised immune response as expected in the mKO-LPS group, demonstrating the protocol's sensitivity in capturing strain-specific mechanistic differences.

General notes and troubleshooting

General notes

1. Sample pooling and dissociation: To minimize inter-animal biological variation, samples from the same treatment group may be pooled into a single gentleMACS C tube. This system accommodates volumes from 500 µL to 10 mL. When attaching the tube to the gentleMACS Dissociator, verify that the tissue is physically positioned within the rotor area to ensure uniform homogenization.
2. If a gentleMACS Octo Dissociator with Heaters is not available, manual incubation can be performed. Between the pre-set dissociation programs, remove the C tube and place it in a 37 °C water bath for 5–10 min with gentle agitation. Ensure the tube is properly re-attached and the tissue remains in the rotor area for each subsequent dissociation cycle.

3. Unique barcoding for multiplexing: In step C5, each biological sample must be labeled with a unique streptavidin-conjugated oligo barcode. Assigning distinct barcodes is the only way to computationally demultiplex individual samples from the shared pool following GEM generation and sequencing.
4. Scaling dead cell removal: During step D2, the volume of dead cell removal microbeads should be maintained as specified for any cell load up to 10^7 cells. For samples exceeding 10^7 cells, scale all reagent and total buffer volumes proportionally to prevent bead saturation and ensure optimal cell viability and recovery.
5. Integration of biological replicates: To ensure statistical rigor in larger studies, it is recommended that at least three biological replicates be used per experimental group. These biological replicates should be processed individually from the tissue dissociation step to the dead cell removal step (sections A–D). Each biological replicate (e.g., three different WT-LPS mice) should be labeled with a unique hashtag oligos (HTOs) during step C5. This enables the computational identification of “inter-individual” vs. “inter-group” variation in downstream analyses.

Troubleshooting

Problem 1: Low cell viability (<70%) after dissociation from step B20.
Possible causes: Excessive mechanical force or over-incubation in enzymes.
Solutions: Reduce the duration of the compression cycles in the gentleMACS program or ensure enzymes are kept on ice until the moment of use.

Problem 2: Low cell recovery after the MS column from step D12.
Possible causes: Cell clumping or column clogging.
Solutions: Ensure the cell suspension is filtered through a 40 μm strainer immediately before applying to the column (step D5). If clogging occurs, use a larger (LS) column.

Problem 3: High percentage of dead cells after MACS separation from step D13.
Possible cause: Reagent volume was scaled down for low cell counts.
Solution: Always use 100 μL of beads for any cell load up to 10^7 cells. Do not scale down, as binding kinetics require a minimum concentration of colloidal beads.

Acknowledgments

Z.Q. and G.X. conceived and designed the study, led and contributed to all aspects of the analysis, and edited the manuscript. F.G. analyzed the data and wrote the manuscript. X.L. and F.S. performed and analyzed all the experimental assays. Y.X. contributed to mouse clone maintenance. The study is supported in part by the NIH National Institute of General Medical Sciences (NIGMS) grant R01 GM144890, National Cancer Institute (NCI) grant R01 CA258614, National Heart, Lung, and Blood Institute R01 HL177140, American Cancer Society (ACS) Research Scholar grant RSG-19-166-01-TBG, American Lung Association (ALA) Lung Cancer Discovery Award 821321, and Tobacco Related-Disease Research Program (TRDRP) Research Award T33IR6461. We also thank other team members for their critical reading and edits.

Competing interests

The authors declare that they have no competing interests.

Ethical considerations

All animal studies were approved by the Institutional Animal Care and Use Committee of the University of Pittsburgh and the University of Southern California and carried out in accordance with NIH guidelines on animal care.

Received: February 5, 2026; Accepted: March 23, 2026; Available online: April 12, 2026; Published: May 05, 2026

References

1. Tang, F., Barbacioru, C., Wang, Y., Nordman, E., Lee, C., Xu, N., Wang, X., Bodeau, J., Tuch, B. B., Siddiqui, A., et al. (2009). mRNA-Seq whole-transcriptome analysis of a single cell. *Nat Methods.* 6(5): 377–382. https://doi.org/10.1038/nmeth.1315
2. Peterson, V. M., Zhang, K. X., Kumar, N., Wong, J., Li, L., Wilson, D. C., Moore, R., McClanahan, T. K., Sadekova, S., Klappenbach, J. A., et al. (2017). Multiplexed quantification of proteins and transcripts in single cells. *Nat Biotechnol.* 35(10): 936–939. https://doi.org/10.1038/nbt.3973
3. Shahi, P., Kim, S. C., Haliburton, J. R., Gartner, Z. J. and Abate, A. R. (2017). Abseq: Ultrahigh-throughput single cell protein profiling with droplet microfluidic barcoding. *Sci Rep.* 7(1): e1038/srep44447. https://doi.org/10.1038/srep44447
4. Stoeckius, M., Hafemeister, C., Stephenson, W., Houck-Loomis, B., Chattopadhyay, P. K., Swerdlow, H., Satija, R. and Smibert, P. (2017). Simultaneous epitope and transcriptome measurement in single cells. *Nat Methods.* 14(9): 865–868. https://doi.org/10.1038/nmeth.4380
5. Stoeckius, M., Zheng, S., Houck-Loomis, B., Hao, S., Yeung, B. Z., Mauck, W. M., Smibert, P. and Satija, R. (2018). Cell Hashing with barcoded antibodies enables multiplexing and doublet detection for single cell genomics. *Genome Biol.* 19(1): e1186/s13059–018–1603–1. https://doi.org/10.1186/s13059-018-1603-1
6. McGinnis, C. S., Patterson, D. M., Winkler, J., Conrad, D. N., Hein, M. Y., Srivastava, V., Hu, J. L., Murrow, L. M., Weissman, J. S., Werb, Z., et al. (2019). MULTI-seq: sample multiplexing for single-cell RNA sequencing using lipid-tagged indices. *Nat Methods.* 16(7): 619–626. https://doi.org/10.1038/s41592-019-0433-8
7. Gao, F., Liu, X., Sun, F., Xiao, Y., Xiao, G. and Qu, Z. (2025). Myeloid *PDLIM2* repression as a common mechanism of infection susceptibility in lung diseases. *Front Immunol.* 16: e1669117. https://doi.org/10.3389/fimmu.2025.1669117
8. Torrado, M., Senatorov, V. V., Trivedi, R., Fariss, R. N. and Tomarev, S. I. (2004). Pdlim2, a Novel PDZ–LIM Domain Protein, Interacts with α-Actinins and Filamin A. *Investigative Opthalmology & Visual Science* 45(11): 3955. https://doi.org/10.1167/iovs.04-0721
9. Loughran, G., Healy, N. C., Kiely, P. A., Huigsloot, M., Kedersha, N. L. and O'Connor, R. (2005). Mystique Is a New Insulin-like Growth Factor-I-regulated PDZ-LIM Domain Protein That Promotes Cell Attachment and Migration and Suppresses Anchorage-independent Growth. *Mol Biol Cell.* 16(4): 1811–1822. https://doi.org/10.1091/mbc.e04-12-1052
10. Tanaka, T., Soriano, M. A. and Grusby, M. J. (2005). SLIM Is a Nuclear Ubiquitin E3 Ligase that Negatively Regulates STAT Signaling. *Immunity.* 22(6): 729–736. https://doi.org/10.1016/j.immuni.2005.04.008
11. Sun, F., Li, L., Yan, P., Zhou, J., Shapiro, S. D., Xiao, G. and Qu, Z. (2019). Causative role of *PDLIM2* epigenetic repression in lung cancer and therapeutic resistance. *Nat Commun.* 10(1): e1038/s41467–019–13331–x. https://doi.org/10.1038/s41467-019-13331-x
12. Gao, F., Xiao, Y., Zhang, H., Shapiro, S. D., Qu, Z. and Xiao, G. (2025). *PDLIM2* in Lung Adenocarcinoma Metastasis. *bioRxiv*: e692242. https://doi.org/10.64898/2025.12.03.692242
13. Gao, F., Chen, Y. W., Shapiro, S. D., Xiao, G. and Qu, Z. (2026). PDLIM2 repression: a common mechanism in viral lung infection. ImmunoHorizons 10(3). https://doi.org/10.1093/immhor/vlag010
14. Li, L., Sun, F., Han, L., Liu, X., Xiao, Y., Gregory, A. D., Shapiro, S. D., Xiao, G. and Qu, Z. (2021). PDLIM2 repression by ROS in alveolar macrophages promotes lung tumorigenesis. *JCI Insight.* 6(5): e144394. https://doi.org/10.1172/jci.insight.144394
15. Zhang, H., Xiao, Y., Gao, F., Le, T. H., Shapiro, S. D., Xiao, G. and Qu, Z. (2026). Alveolar epithelial NF-κB/RelA guards the lung against bacterial infection. *J Immunol.* 215(2): e1093/jimmun/vkaf374. https://doi.org/10.1093/jimmun/vkaf374
16. Sun, F., Yan, P., Xiao, Y., Zhang, H., Shapiro, S. D., Xiao, G. and Qu, Z. (2024). Improving PD-1 blockade plus chemotherapy for complete remission of lung cancer by nanoPDLIM2. *eLife.* 12: e89638. https://doi.org/10.7554/elife.89638
17. Sun, F., Guo, Z. S., Gregory, A. D., Shapiro, S. D., Xiao, G. and Qu, Z. (2020). Dual but not single PD-1 or TIM-3 blockade enhances oncolytic virotherapy in refractory lung cancer. *J ImmunoTher Cancer.* 8(1): e000294. https://doi.org/10.1136/jitc-2019-000294
18. Sun, F., Li, L., Xiao, Y., Gregory, A. D., Shapiro, S. D., Xiao, G. and Qu, Z. (2021). Alveolar Macrophages Inherently Express Programmed Death-1 Ligand 1 for Optimal Protective Immunity and Tolerance. *J Immunol.* 207(1): 110–114. https://doi.org/10.4049/jimmunol.2100046

19. Ashouri, K., Krause, H., Elliott, A., Liu, S. V., Ma, P. C., Halmos, B., Qu, Z., Xiao, G., Vanderwalde, A., Nieva, J. J., et al. (2024). Abstract 5201: Characterization of *PDLIM2* in non-small cell lung cancer. *Cancer Res.* 84: 5201–5201. https://doi.org/10.1158/1538-7445.am2024-5201
20. Yan, P., Qu, Z., Ishikawa, C., Mori, N. and Xiao, G. (2009). Human T-Cell Leukemia Virus Type I-Mediated Repression of PDZ-LIM Domain-Containing Protein 2 Involves DNA Methylation But Independent of the Viral Oncoprotein Tax. *Neoplasia*. 11(10): 1036–1041. https://doi.org/10.1593/neo.09752
21. Qu, Z., Fu, J., Yan, P., Hu, J., Cheng, S. Y. and Xiao, G. (2010). Epigenetic Repression of PDZ-LIM Domain-containing Protein 2. *J Biol Chem.* 285(16): 11786–11792. https://doi.org/10.1074/jbc.m109.086561
22. Qu, Z., Yan, P., Fu, J., Jiang, J., Grusby, M. J., Smithgall, T. E. and Xiao, G. (2010). DNA Methylation–Dependent Repression of PDZ-LIM Domain–Containing Protein 2 in Colon Cancer and Its Role as a Potential Therapeutic Target. *Cancer Res.* 70(5): 1766–1772. https://doi.org/10.1158/0008-5472.can-09-3263
23. Guo, Z. S. and Qu, Z. (2021). PDLIM2: Signaling pathways and functions in cancer suppression and host immunity. *Biochim Biophys Acta Rev Cancer*. 1876(2): 188630. https://doi.org/10.1016/j.bbcan.2021.188630
24. Sun, F., Xiao, G. and Qu, Z. (2024). PDLIM2 is a novel E5 ubiquitin ligase enhancer that stabilizes ROC1 and recruits the ROC1-SCF ubiquitin ligase to ubiquitinate and degrade NF-κB RelA. *Cell Biosci.* 14(1): e1186/s13578–024–01281–x. https://doi.org/10.1186/s13578-024-01281-x
25. Qu, Z., Qing, G., Rabson, A. and Xiao, G. (2004). Tax Deregulation of NF-κB2 p100 Processing Involves Both β-TrCP-dependent and -independent Mechanisms. *J Biol Chem.* 279(43): 44563–44572. https://doi.org/10.1074/jbc.m403689200
26. Tanaka, T., Grusby, M. J. and Kaisho, T. (2007). PDLIM2-mediated termination of transcription factor NF-κB activation by intranuclear sequestration and degradation of the p65 subunit. *Nat Immunol.* 8(6): 584–591. https://doi.org/10.1038/ni1464
27. Tanaka, T., Yamamoto, Y., Muromoto, R., Ikeda, O., Sekine, Y., Grusby, M. J., Kaisho, T. and Matsuda, T. (2011). PDLIM2 Inhibits T Helper 17 Cell Development and Granulomatous Inflammation Through Degradation of STAT3. *Sci Signaling*. 4(202): e2001637. https://doi.org/10.1126/scisignal.2001637
28. Qu, Z., Fu, J., Ma, H., Zhou, J., Jin, M., Mapara, M. Y., Grusby, M. J. and Xiao, G. (2012). PDLIM2 restricts Th1 and Th17 differentiation and prevents autoimmune disease. *Cell Biosci.* 2(1): e1186/2045–3701–2–23. https://doi.org/10.1186/2045-3701-2-23
29. Sun, F., Xiao, Y. and Qu, Z. (2015). Oncovirus Kaposi Sarcoma Herpesvirus (KSHV) Represses Tumor Suppressor PDLIM2 to Persistently Activate Nuclear Factor κB (NF-κB) and STAT3 Transcription Factors for Tumorigenesis and Tumor Maintenance. *J Biol Chem.* 290(12): 7362–7368. https://doi.org/10.1074/jbc.c115.637918
30. Vanoirbeek, E., Eelen, G., Verlinden, L., Carmeliet, G., Mathieu, C., Bouillon, R., O'Connor, R., Xiao, G. and Verstuyf, A. (2013). PDLIM2 expression is driven by vitamin D and is involved in the pro-adhesion, and anti-migration and -invasion activity of vitamin D. *Oncogene.* 33(15): 1904–1911. https://doi.org/10.1038/onc.2013.123
31. Yan, P., Fu, J., Qu, Z., Li, S., Tanaka, T., Grusby, M. J. and Xiao, G. (2009). PDLIM2 suppresses human T-cell leukemia virus type I Tax-mediated tumorigenesis by targeting Tax into the nuclear matrix for proteasomal degradation. *Blood.* 113(18): 4370–4380. https://doi.org/10.1182/blood-2008-10-185660
32. Fu, J., Yan, P., Li, S., Qu, Z. and Xiao, G. (2010). Molecular determinants of PDLIM2 in suppressing HTLV-I Tax-mediated tumorigenesis. *Oncogene.* 29(49): 6499–6507. https://doi.org/10.1038/onc.2010.374
33. XIAO, G., RABSON, A., YOUNG, W., QING, G. and QU, Z. (2006). Alternative pathways of NF-κB activation: A double-edged sword in health and disease. *Cytokine Growth Factor Rev.* 17(4): 281–293. https://doi.org/10.1016/j.cytogfr.2006.04.005
34. XIAO, G. (2007). Autophagy and NF-κB: Fight for fate. *Cytokine & Growth Factor Reviews* 18: 233–243. https://doi.org/10.1016/j.cytogfr.2007.04.006
35. Qu, Z. and Xiao, G. (2011). Human T-Cell Lymphotropic Virus: A Model of NF-κB-Associated Tumorigenesis. *Viruses.* 3(6): 714–749. https://doi.org/10.3390/v3060714
36. Xiao, G. and Fu, J. (2011). NF-kappaB and cancer: a paradigm of Yin-Yang. *Am J Cancer Res.* 1(2): 192-221. https://www.ncbi.nlm.nih.gov/pubmed/21969033.
37. Li, L., Han, L., Sun, F., Zhou, J., Ohaegbulam, K. C., Tang, X., Zang, X., Steinbrecher, K. A., Qu, Z., Xiao, G., et al. (2018). NF-κB RelA renders tumor-associated macrophages resistant to and capable of directly suppressing $CD8^{+}$T cells for tumor promotion. *Oncoimmunology.* 7(6): e1435250. https://doi.org/10.1080/2162402x.2018.1435250
38. Li, L., Han, L. and Qu, Z. (2024). NF-κB RelA is a cell-intrinsic metabolic checkpoint restricting glycolysis. *Cell Biosci.* 14(1): e1186/s13578–024–01196–7. https://doi.org/10.1186/s13578-024-01196-7
39. Xiao, G. and Sun, S. C. (2001). Negative regulation of the nuclear factor κB-inducing kinase by a cis-acting domain. *J Biol Chem.* 276(9): 6879. https://doi.org/10.1074/s0021-9258(19)34707-6

40. Xiao, G., Harhaj, E. W. and Sun, S. C. (2000). Domain-specific Interaction with the IκB Kinase (IKK) Regulatory Subunit IKKγ Is an Essential Step in Tax-mediated Activation of IKK. *J Biol Chem.* 275(44): 34060–34067. https://doi.org/10.1074/jbc.m002970200
41. Xiao, G. and Sun, S. C. (2000). Activation of IKKα and IKKβ through their fusion with HTLV-I Tax protein. *Oncogene.* 19(45): 5198–5203. https://doi.org/10.1038/sj.onc.1203894
42. Senftleben, U., Cao, Y., Xiao, G., Greten, F. R., Krähn, G., Bonizzi, G., Chen, Y., Hu, Y., Fong, A., Sun, S. C., et al. (2001). Activation by IKKα of a Second, Evolutionary Conserved, NF-κB Signaling Pathway. *Science (1979).* 293(5534): 1495–1499. https://doi.org/10.1126/science.1062677
43. Xiao, G. (2001). Retroviral oncoprotein Tax induces processing of NF-kappaB2/p100 in T cells: evidence for the involvement of IKKalpha. *EMBO J.* 20(23): 6805–6815. https://doi.org/10.1093/emboj/20.23.6805
44. Xiao, G., Harhaj, E. W. and Sun, S. C. (2001). NF-κB-Inducing Kinase Regulates the Processing of NF-κB2 p100. *Mol Cell.* 7(2): 401–409. https://doi.org/10.1016/s1097-2765(01)00187-3
45. Qing, G., Qu, Z. and Xiao, G. (2005). Regulation of NF-κB2 p100 Processing by Its cis-Acting Domain. *J Biol Chem.* 280(1): 18–27. https://doi.org/10.1074/jbc.m406619200
46. Qing, G., Qu, Z. and Xiao, G. (2005). Stabilization of Basally Translated NF-κB-inducing Kinase (NIK) Protein Functions as a Molecular Switch of Processing of NF-κB2 p100. *J Biol Chem.* 280(49): 40578–40582. https://doi.org/10.1074/jbc.m508776200
47. Qing, G. and Xiao, G. (2005). Essential Role of IκB Kinase α in the Constitutive Processing of NF-κB2 p100. *J Biol Chem.* 280(11): 9765–9768. https://doi.org/10.1074/jbc.c400502200
48. Xiao, G., Fong, A. and Sun, S. C. (2004). Induction of p100 Processing by NF-κB-inducing Kinase Involves Docking IκB Kinase α (IKKα) to p100 and IKKα-mediated Phosphorylation. *J Biol Chem.* 279(29): 30099–30105. https://doi.org/10.1074/jbc.m401428200
49. Arabi, A., Ullah, K., Branca, R. M., Johansson, J., Bandarra, D., Haneklaus, M., Fu, J., Ariës, I., Nilsson, P., Den Boer, M. L., et al. (2012). Proteomic screen reveals Fbw7 as a modulator of the NF-κB pathway. *Nat Commun.* 3(1): e1038/ncomms1975. https://doi.org/10.1038/ncomms1975
50. Song, X. and Qu, Z. (2024). NF-κB1 deficiency promotes macrophage-derived adrenal tumors but decreases neurofibromas in HTLV-I LTR-Tax transgenic mice. *PLoS One.* 19(5): e0303138. https://doi.org/10.1371/journal.pone.0303138
51. Sun, F., Qu, Z., Xiao, Y., Zhou, J., Burns, T. F., Stabile, L. P., Siegfried, J. M. and Xiao, G. (2015). NF-κB1 p105 suppresses lung tumorigenesis through the Tpl2 kinase but independently of its NF-κB function. *Oncogene.* 35(18): 2299–2310. https://doi.org/10.1038/onc.2015.299
52. Qing, G., Qu, Z. and Xiao, G. (2007). Endoproteolytic processing of C-terminally truncated NF-κB2 precursors at κB-containing promoters. *Proc Natl Acad Sci USA.* 104(13): 5324–5329. https://doi.org/10.1073/pnas.0609914104
53. Sun, F., Xiao, Y., Shapiro, S. D., Qu, Z. and Xiao, G. (2024). Critical and distinct roles of cell type–specific NF-κB2 in lung cancer. *JCI Insight.* 9(4): e164188. https://doi.org/10.1172/jci.insight.164188
54. Fu, J., Qu, Z., Yan, P., Ishikawa, C., Aqeilan, R. I., Rabson, A. B. and Xiao, G. (2011). The tumor suppressor gene WWOX links the canonical and noncanonical NF-κB pathways in HTLV-I Tax-mediated tumorigenesis. *Blood.* 117(5): 1652–1661. https://doi.org/10.1182/blood-2010-08-303073
55. Yan, P., Qing, G., Qu, Z., Wu, C. C., Rabson, A. and Xiao, G. (2007). Targeting Autophagic Regulation of NF-kappaB in HTLV-I Transformed Cells by Geldanamycin: Implications for Therapeutic Interventions. *Autophagy.* 3(6): 600–603. https://doi.org/10.4161/auto.4761
56. Qing, G., Yan, P. and Xiao, G. (2006). Hsp90 inhibition results in autophagy-mediated proteasome-independent degradation of IκB kinase (IKK). *Cell Res.* 16(11): 895–901. https://doi.org/10.1038/sj.cr.7310109
57. Qing, G., Yan, P., Qu, Z., Liu, H. and Xiao, G. (2007). Hsp90 regulates processing of NF-κB2 p100 involving protection of NF-κB-inducing kinase (NIK) from autophagy-mediated degradation. *Cell Res.* 17(6): 520–530. https://doi.org/10.1038/cr.2007.47
58. Zhou, J., Qu, Z., Yan, S., Sun, F., Whitsett, J. A., Shapiro, S. D. and Xiao, G. (2014). Differential roles of STAT3 in the initiation and growth of lung cancer. *Oncogene.* 34(29): 3804–3814. https://doi.org/10.1038/onc.2014.318
59. Qu, Z., Sun, F., Zhou, J., Li, L., Shapiro, S. D. and Xiao, G. (2015). Interleukin-6 Prevents the Initiation but Enhances the Progression of Lung Cancer. *Cancer Res.* 75(16): 3209–3215. https://doi.org/10.1158/0008-5472.can-14-3042
60. Zhou, J., Qu, Z., Sun, F., Han, L., Li, L., Yan, S., Stabile, L. P., Chen, L. F., Siegfried, J. M., Xiao, G., et al. (2017). Myeloid STAT3 Promotes Lung Tumorigenesis by Transforming Tumor Immunosurveillance into Tumor-Promoting Inflammation. *Cancer Immunol Res.* 5(3): 257–268. https://doi.org/10.1158/2326-6066.cir-16-0073

61. Chen, M., Sun, F., Han, L. and Qu, Z. (2016). Kaposi's sarcoma herpesvirus (KSHV) microRNA K12-1 functions as an oncogene by activating NF-κB/IL-6/STAT3 signaling. *Oncotarget.* 7(22): 33363–33373. https://doi.org/10.18632/oncotarget.9221
62. Sun, F., Qu, Z. and Xiao, G. (2021). Methods to Detect NF-κB Activity in Tumor-Associated Macrophage (TAM) Populations. *Methods Mol Biol.* 213–241. https://doi.org/10.1007/978-1-0716-1669-7_13
63. Qu, Z. and Xiao, G. (2015). Systematic Detection of Noncanonical NF-κB Activation. *Methods Mol Biol.* : 121–154. https://doi.org/10.1007/978-1-4939-2422-6_8
64. Sun, F., Xiao, G. and Qu, Z. (2017). Murine Bronchoalveolar Lavage. *Bio Protoc.* 7(10): e2287. https://doi.org/10.21769/bioprotoc.2287
65. Sun, F., Xiao, G. and Qu, Z. (2017). Isolation of Murine Alveolar Type II Epithelial Cells. *Bio Protoc.* 7(10): e2288. https://doi.org/10.21769/bioprotoc.2288
66. Le, T., Sun, F., Xiao, G. and Qu, Z. (2025). Nano*PDLIM2*-Based Combination Therapy for Lung Cancer Treatment in Mouse Preclinical Studies. *Bio Protoc.* 15(1379): e5437. https://doi.org/10.21769/bioprotoc.5437